JOURNAL OF GEOPHYSICAL RESEARCH, VOL. 117, C07015, doi:10.1029/2012JC007968, 2012

The forcing mechanism leading to the Kuroshio intrusion into the South China Sea

Chau-Ron Wu[1] and Yi-Chia Hsin[2]

Received 7 February 2012; revised 25 May 2012; accepted 4 June 2012; published 19 July 2012.

[1] We use a high-resolution numerical model to examine the forcing mechanism responsible for Kuroshio intrusion into the South China Sea (SCS). The collective wisdom is that variations in Kuroshio intrusion are closely related to the wind, inside or outside the SCS. A series of experiments was performed to identify the wind-related forcing regulating the intrusion. The experiments demonstrated that the importance of wind inside the SCS is greater than that outside the SCS. Furthermore, the northwestward Ekman drift due to northeasterly wind in winter intensifies the upstream Kuroshio in the Luzon Strait, enhancing the Kuroshio intrusion into the SCS. In particular, the wind stress curl (WSC) off southwest Taiwan is chiefly responsible for the Kuroshio intrusion. Both the WSC and intrusion show both seasonal and intraseasonal variation. As the negative WSC off southwest Taiwan becomes stronger, it contributes to anticyclonic circulation. The enhanced anticyclonic circulation helps the development of the Kuroshio intrusion. The consistency between WSC variability and the intrusion suggests that the WSC off southwest Taiwan is essential to the Kuroshio intrusion variability.

Citation: Wu, C.-R., and Y.-C. Hsin (2012), The forcing mechanism leading to the Kuroshio intrusion into the South China Sea, *J. Geophys. Res.*, *117*, C07015, doi:10.1029/2012JC007968.

1. Introduction

[2] Luzon Strait is a gap in the western boundary of the North Pacific Ocean. The northward-flowing Kuroshio tends to loop within the Luzon Strait before continuing northward off east Taiwan [e.g., *Shaw*, 1991; *Qu et al.*, 2000]. Based on satellite data and numerical model output, *Nan et al.* [2011] demonstrated that the Kuroshio intrusion has three typical paths: looping, leaking, and leaping. Various observations have shown that the degree of the loop (or the Kuroshio intrusion) varies seasonally [e.g., *Centurioni et al.*, 2004; *Liang et al.*, 2008]. In general, the Kuroshio tends to bypass the Luzon Strait in summer without significant westward encroachment. In winter, the Kuroshio often makes a larger meander, and the intrusion is not confined within the Luzon Strait but penetrates into the South China Sea (SCS). For example, based on hydrographic data, *Shaw* [1991] suggested that Kuroshio intrusion water can reach west of 117°E along the continental slope in winter, but most of the intrusion water is restricted to the area farther east in summer. During the period of 1989∼2002, drifters were found to enter the SCS between October and December, whereas no drifters were found inside the SCS between July and September [*Centurioni et al.*, 2004].

[3] The Kuroshio encroachment does not occur within the entire Luzon Strait. The largest westward intrusion occurs at the Balintang Channel and the south of Babuyan Island [*Liang et al.*, 2003; *Centurioni et al.*, 2004]. The mechanism leading to Kuroshio intrusion into the SCS has drawn considerable attention. Based on observations, *Farris and Wimbush* [1996] demonstrated that local winds directly affect the Kuroshio intrusion, and the time-integrated wind stress in the Luzon Strait dominates the expansion of the Kuroshio loop. Numerical experiments by *Metzger and Hurlburt* [1996] attributed the seasonal variation in Luzon Strait transport to the pileup of waters by monsoon winds both inside and outside the SCS. *Jia and Chassignet* [2011] also confirmed the significance of the local winds and further quantified their effects. They found that when the integrated Ekman transport exceeds 2×10^{12} m^3 (roughly the volume of an eddy), the Kuroshio loop expands, and an eddy-shedding event occurs within one month [*Jia and Chassignet*, 2011]. *Hsin et al.* [2012] conducted a series of elimination experiments to assess the relative importance of open-ocean inflow/outflow, wind stress, and surface heat flux in the regulation of Luzon Strait transport and its seasonality. Their analysis showed that the monsoon wind is the dominant driving mechanism regulating the strength of upper-ocean Luzon Strait transport.

[4] *Metzger and Hurlburt* [2001b] suggested that the stronger negative wind stress curl in the northern Luzon

[1]Department of Earth Sciences, National Taiwan Normal University, Taipei, Taiwan.
[2]Department of Oceanography, University of Hawai'i at Mānoa, Honolulu, Hawaii, USA.

Corresponding author: C.-R. Wu, Department of Earth Sciences, National Taiwan Normal University, 88, Section 4 Ting-Chou Rd., Taipei 11677, Taiwan. (cwu@ntnu.edu.tw)

0148-0227/12/2012JC007968

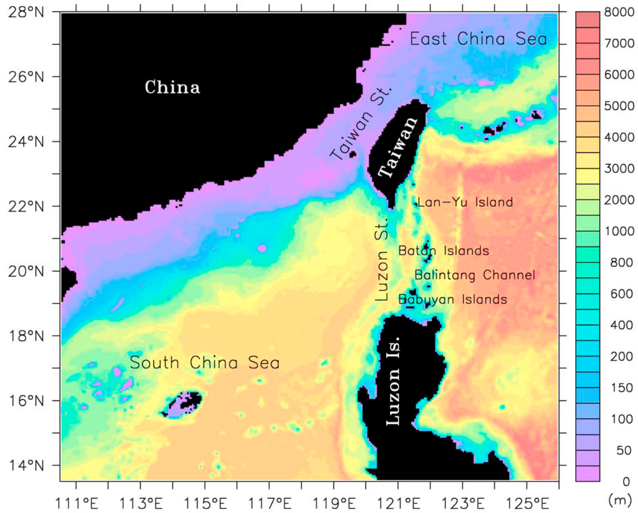

Figure 1. Seas Around Taiwan (SAT) model domain and bathymetry.

Strait increases Ekman pumping, deepening the thermocline and enhancing the westward Kuroshio intrusion. Based on an idealized model, *Sheremet* [2001] concluded that the intensity of the upstream flow (the Kuroshio off east Luzon) determines whether the current can intrude into a gap. *Qu* [2000] suggested that the degree of Kuroshio intrusion could be associated with the meridional pressure gradient across the Luzon Strait. *Liang et al.* [2008] further noted this meridional pressure gradient can be attributed to the local wind stress curl west of Luzon Island. However, *Metzger and Hurlburt* [2001a] demonstrated that small changes in the island and coastline representation in the Luzon Strait can have a large influence on the intrusive pathway of the Kuroshio.

[5] In summary, most of these studies have noted that variation in the Kuroshio intrusion is closely related to the wind. However, it is still unclear whether the wind or wind curl is the more important factor. Additionally, it is unclear whether winds inside or outside the SCS (or both) are the dominant forcing for the intrusion. To answer these questions, we performed several model experiments. Results based on a nested three-dimensional, primitive-equation numerical ocean model were analyzed to describe the varying degree of the Kuroshio intrusion. With finer model grids, refined topography representation, and improved temporal resolution in atmospheric forcing, our work elucidates a reasonable mechanism for the westward intrusion. Section 2 describes the observation-validated model. Section 3 uses a series of model experiments to identify the wind-related forcing regulating the Kuroshio intrusion. Section 4 presents a discussion of the temporal variability in the wind stress curl and its effect on the intrusion. Concluding remarks are given in Section 5.

2. Model Description

[6] The Seas Around Taiwan (SAT) model used in this study is based on the sigma-coordinate Princeton Ocean Model (POM) [*Mellor*, 2004]. On the basis of hydrostatic approximation, this model solves three-dimensional primitive equations for the momentum, salt, and heat, and evaluates turbulence by the level 2.5 Mellor-Yamada scheme. Figure 1 shows the SAT model domain, 110.5°E∼126°E and 13.5°N∼28°N, and its bottom topography. The horizontal grid size is 1/20° and there are 26 vertical sigma levels. The topography of the SAT model is a blend of the 1/30° × 1/30° TaiDBMv6 (Ocean Data Bank, Nation Center for Ocean Research, Taiwan) and 1/12° × 1/12° ETOPO5 (National Geophysical Data Center, National Oceanic and Atmospheric Administration, National Environmental Satellite, Data and Information Service, USA) bathymetric data. We interpolated the model bathymetry mainly from TaiDBMv6, especially for the region around Taiwan. The islands around the Luzon Strait are well represented in this blended data set (Figure 1). A larger-scale East Asian Marginal Seas model (EAMS) is used to serve the mean inflow/outflow averaged over 2000∼2008 on the open boundaries of the SAT model. The EAMS model, extending from 99°E to 140°E and from 0°N to 42°N, has a horizontal resolution of 1/8° and also 26 sigma levels. A detailed description of the EAMS model has been given by *Hsin et al.* [2008]. The EAMS model was able to reproduce flow patterns of Taiwan Strait currents [*Wu and Hsin*, 2005] and variations of the Kuroshio east of Taiwan and around Luzon Strait [*Hsin et al.*, 2008, 2010, 2012; *Sheu et al.*, 2010].

[7] The SAT model forced by QuikSCAT/NCEP blended wind product (http://dss.ucar.edu) has been used to investigate the spatiotemporal variability of the cold dome off northeastern Taiwan [*Wu et al.*, 2008]. The validations and more detailed descriptions of the SAT model are given in *Wu et al.* [2008]. To reach the purpose of this study, the SAT model is spun up for 500 days, and then driven by the 6-hourly 0.5° × 0.5° QuikSCAT/NCEP blended wind product from 1 January 2000 to 31 December 2001. We choose this period because there are two subsurface moorings deployed in the vicinity during the time span, and the two-year model outputs are adopted for later analysis. Several model experiments were performed from the same initial state using the SAT model, but with different wind-forcing domain and intensity. All model experiments are summarized in Table 1. Experiments 1 and 2 were executed for the same period as CTL. Data from these three experiments

Table 1. List of Model Experiments

Experiment	Descriptions
CTL	Forced by annual mean lateral boundary conditions and 6-hourly QuikSCAT/NCEP wind stress.
EX1	Same as CTL, but wind domain covers only *east* of the yellow line in Figure 4a.
EX2	Same as CTL, but wind domain covers only *west* of the yellow line in Figure 4a.
W3	Forced by annual mean lateral boundary conditions and a constant wind stress of -0.3 Nm^{-2}.
W2	Same as W3, but a constant wind stress of -0.2 Nm^{-2}.
W1	Same as W3, but a constant wind stress of -0.1 Nm^{-2}.
C1	Adding -1.6×10^{-6} Nm^{-3} off southwest Taiwan (typical value of wind stress curl in winter) to the homogeneous wind field (shown as Figure 6c).
C2	Same as C1, but -3.2×10^{-6} Nm^{-3} is added.

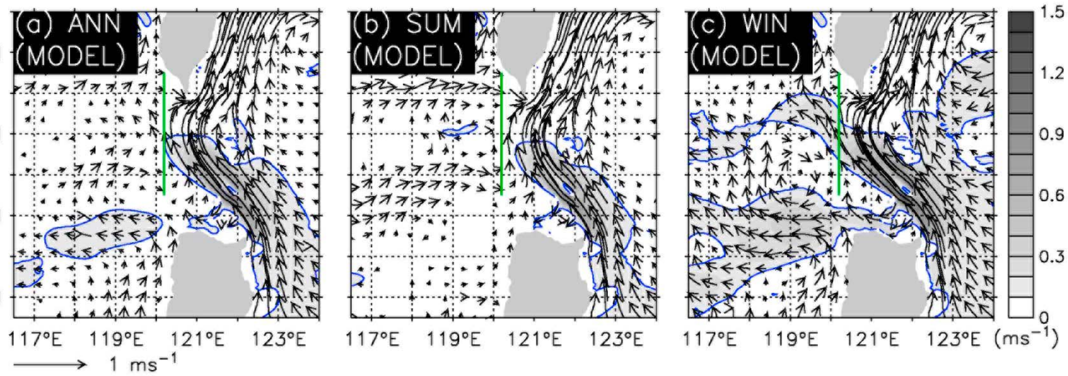

Figure 2. Surface flow pattern for (a) modeled annual mean, (b) modeled summer average, and (c) modeled winter average. Summer and winter are defined as June and December average. Surface current is averaged from 0 to 50 m, and only current speed larger than 0.05 ms^{-1} is plotted. Westward zonal velocity is shaded. Blue curve denotes 0.1 ms^{-1} contour. Green line represents the western limit of 0.1 ms^{-1} isotach of annual mean zonal velocity.

during the period April 2000~December 2001 were used for subsequent discussion. To clarify the relative importance of wind stress and its curl in the Kuroshio intrusion, five additional experiments, W1, W2, W3, C1, and C2, forced by simplified artificial wind fields were performed. These five experiments were run for 500 days, and data averaged over the final 300 days was used for further analysis.

3. Results

3.1. Seasonal Kuroshio Intrusion

[8] Figures 2a–2c show the simulated annual, June, and December averaged circulation patterns. The westward zonal velocity is shaded. The seasonal variation is quite apparent in the figures. A meridional section of ~120°E (green line in Figure 2) denoting the western limit of the Kuroshio intrusion is defined by the westernmost end of the −0.1 ms^{-1} isotach of the annual mean Kuroshio pattern (Figure 2a). Figure 2b shows a typical summer regime. In summer, the southwest monsoon often prevails over the Luzon Strait. After leaving the northern tip of Luzon Island, the northward-flowing Kuroshio enters the vicinity of the Luzon Strait. In the strait, the northward component overwhelms the westward component of the Kuroshio, indicating a relatively straight path. Then, the intrusion is confined within the Luzon Strait east of 120°E. Most of the Kuroshio waters return to the east and continue to flow northward along the east coast of Taiwan. However, the Kuroshio intrusion reaches farthest in winter, extending to 117°E (Figure 2c). Hydrographic data analyses [*Shaw*, 1989, 1991] lend further support to this picture: intrusive Pacific water can be found west of 117°E in winter but farther east in summer. Long-term observations from both surface drifter trajectories [*Centurioni et al.*, 2004] and shipboard Acoustic Doppler Current Profiler (ADCP) velocity composites [*Liang et al.*, 2003] have also confirmed the existence of a Kuroshio meander across the Luzon Strait.

[9] Concurrent geostrophic velocities derived from satellite altimeter sea level anomalies of AVISO (Archiving, Validation, and Interpretation of Satellite Oceanographic data; http://www.aviso.oceanobs.com) plus mean dynamic topography calculated from altimetry and a geoid model [*Rio et al.*, 2009] were analyzed to further validate the model results. The reliability of the altimetry products in the area was tested by *Hsin et al.* [2010], who demonstrated that the altimeter-based geostrophic velocities were comparable to shipboard ADCP velocity composites in the region, but with a weaker magnitude [*Hsin et al.*, 2010, Figure 1]. We also compared the altimeter-based velocities with velocities from two subsurface moorings deployed off southwest Taiwan [*Wu et al.*, 2005]. During the deployed period between August 2000 and August 2001, the geostrophic velocity was generally weaker than that measured by mooring ADCPs, but the velocity tendencies were in close agreement (figures not shown). Figures 3a and 3b show the altimeter-based geostrophic velocity in summer and winter, respectively. These seasonal flow patterns are quite similar to those drawn from model simulations (Figures 2b and 2c). This is particularly true around the Luzon Strait, including the intrusion position and pathway of the Kuroshio. The Kuroshio flows northward in a relatively straight path from east of Luzon to east of Taiwan in summer, where the intrusion is confined within the Luzon Strait (Figure 3a). The encroachment in winter extends to west of 117°E in Figure 3b. The altimetry product also shows a weaker velocity than the model simulation. The magnitude of the model velocity is closer to that measured by both mooring and shipboard ADCPs than is the altimeter-based geostrophic velocity.

3.2. Model Experiments

[10] Although most existing observations show that the Kuroshio encroaches on the Luzon Strait, on some occasions, the intruded water can penetrate into the SCS. Here we focus only on the “stronger and/or larger” westward intrusion, which can significantly impact northern SCS circulation as well as the heat and salt balances of the western Pacific marginal seas. Combining the present model outputs with AVISO geostrophic velocity maps (Figures 2 and 3), we found that the longitude of 120°E could serve as an appropriate index for the definition of the westward Kuroshio intrusion. Along the ~120°E vertical section, an intensified westward velocity core was found at ~20.7°N in December

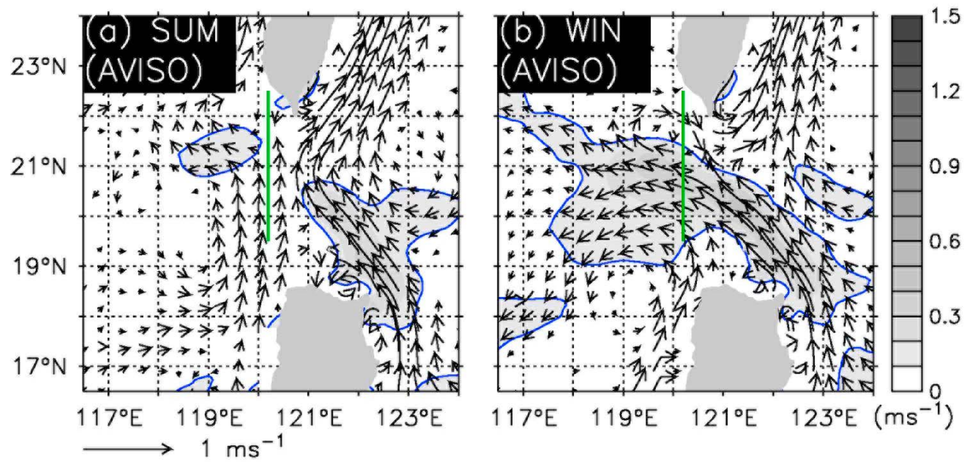

Figure 3. Same as Figure 2 except for altimeter-based (a) summer average and (b) winter average.

as expected, although it was significantly weakened in June (figure not shown).

[11] We conducted two experiments to gain an understanding of the relative importance of winds inside and outside the SCS to the Kuroshio intrusion. In Experiment 1 (EX1), we set the winds to zero west of the yellow line (see Figure 4a) so that they existed only east of the Luzon Strait (east of ~122°E). We chose the yellow line rather than a straight line (e.g., along 120.75°E) across the Luzon Strait. Bursts of artificial wind stress curls appeared when we selected the straight line. The artificial wind stress curls further induced artificial flow in the vicinity of the selected section. The artificial wind stress curls mostly vanished when we chose the yellow line, which is along the island chain of the Luzon Strait. The island chain can be regarded as a "natural" boundary in this study, including Lan-Yu Island, Batan Islands, and Babuyan Islands shown in Figure 1. In Experiment 2 (EX2), we allowed winds only inside the SCS (zero east of the yellow line). During summertime, the flow patterns in the two experiments were similar. The Kuroshio tended to bypass the Luzon Strait, and was confined east of 120°E, without westward intrusion into the SCS (figures not shown). However, a distinct winter pattern was apparent between the two experiments. Figure 4 shows a monthly mean flow pattern in winter for EX1 and EX2. No westward intrusion into the SCS was found in EX1 (Figure 4a), whereas in EX2, the westward intrusion was evident (Figure 4b). The winter intrusion pattern of EX2 was similar to that in the control run (CTL), indicating that EX2 produces a more realistic flow pattern than does EX1. These two experiments demonstrate that wind inside the SCS is relatively important for the Kuroshio intrusion into the SCS.

[12] Further evidence has been seen in the modeled zonal velocity (U) of the western Kuroshio edge and the depth-averaged kinetic energy ($KE = \int_{z=-200}^{z=0} \frac{u^2 + v^2}{2} dz$) of

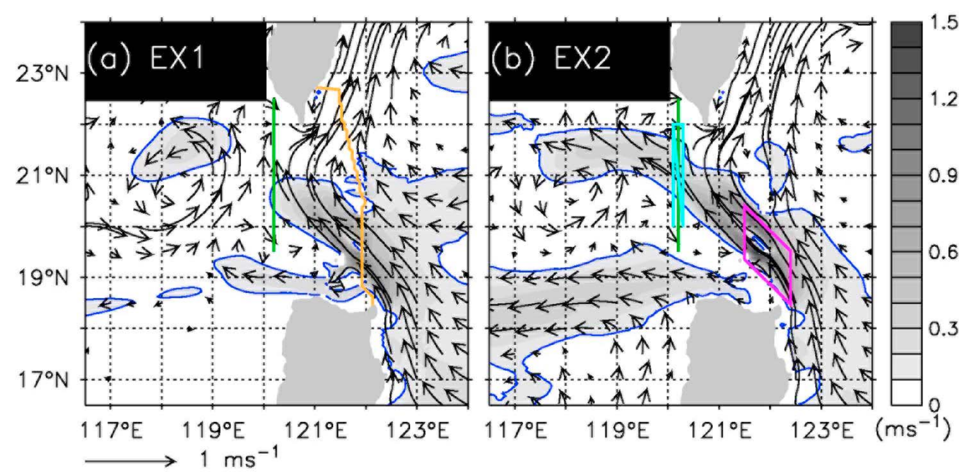

Figure 4. Winter average surface flow patterns for (a) Experiment 1 and (b) Experiment 2. Surface current is averaged from 0 to 50 m, and only current speed larger than 0.05 ms^{-1} is plotted. Green line is the same as that in Figure 2. Yellow line in Figure 4a represents the boundary dividing the wind field into east and west. Blue and purple frames in Figure 4b are the areas for calculating the zonal velocity and kinetic energy anomaly in Figure 5, respectively.

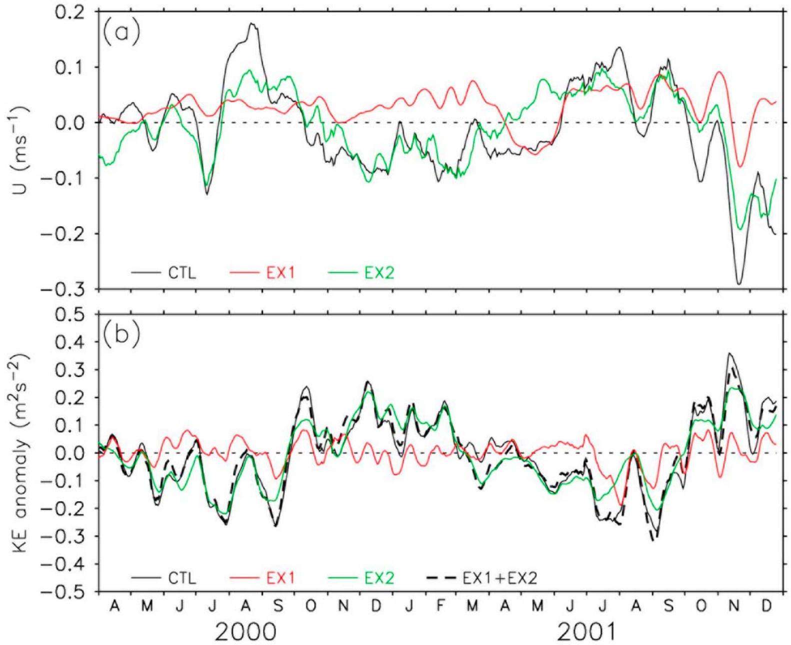

Figure 5. Time series of (a) modeled depth-averaged zonal velocity (0–50 m) and (b) depth-averaged kinetic energy anomaly (0–200 m) of the upstream Kuroshio for the control run (black solid line), EX1 (red), and EX2 (green). In Figure 5b, black dashed line represents the summation of EX1 and EX2. Anomalies are with respect to 0.50, 0.45, and 0.50 for CTL, EX1, and EX2, respectively.

the upstream Kuroshio during the period from April 2000 to December 2001 (Figures 5a and 5b). Blue and purple frames in Figure 4b show the areas for calculating the zonal velocity and KE anomaly, respectively. Both the U and KE anomaly of CTL reveal obvious intraseasonal and seasonal variations, demonstrating that the Kuroshio intrusion contains seasonal and intraseasonal variability. Furthermore, the time series of U and KE anomalies simulated in EX2 are nearly in phase with those in CTL for most of the period. However, the time series of both the U and KE anomalies simulated by EX1 are unrelated to those simulated by CTL. On seasonal time scales, U is large and negative (toward the west) in winter when KE anomalies are positive (enhanced). A similar tendency is also present on intraseasonal timescales. The correlation coefficient (R) between U and KE anomaly is -0.67. The results confirm that the Kuroshio intrusion often occurs during wintertime and demonstrate that the upstream Kuroshio intensity is related to the intrusion.

[13] The monsoonal variability appears to be responsible for the upstream Kuroshio intensity. The northeast wind prevails during wintertime and is favorable for the Kuroshio intrusion. Figure 6a illustrates the mean wintertime wind field derived from the QuikSCAT/NCEP blended wind product, averaged over November–January during the 9-year period from 2000 to 2008. The magnitude of wintertime wind stress was about 0.2 Nm^{-2} toward the southwest, with a standard deviation of about 0.1 Nm^{-2}. One notable feature is the large negative wind stress curl off southwest Taiwan (about -1.6×10^{-6} Nm^{-3}). We decided to leave the influence of the wind stress curl to later model experiments, and we set up a constant wintertime wind stress (-0.2 Nm^{-2}) without curl (Figure 6b) to investigate the influence of the wind stress on the Kuroshio intrusion alone. The simplified artificial wind field is homogeneous over the entire model domain. We then design experiments W3, W2, and W1 with constant wind stress of -0.3, -0.2, and -0.1 Nm^{-2}, respectively, to explore the wind-intensity effect. As expected, the larger Kuroshio intrusion is associated with greater wind stress (Figures 7a–7c). The KE of the upstream Kuroshio in the Luzon Strait also becomes larger as the wind strengthens. The northwestward Ekman drift due to the northeasterly wind in winter enhances the upstream Kuroshio in the Luzon Strait, enriching the Kuroshio intrusion into the SCS. Additionally, a stronger wind also forms a strong anticyclonic eddy centered at 19°N and 119°E inside the SCS. This anticyclonic eddy does not contribute much to the major Kuroshio intrusion in the Balintang Channel. Furthermore, winds with magnitude 0.2 Nm^{-2} are regarded as a typical winter monsoon. Even so, Figure 7b shows no visual westward intrusion (into the SCS) in winter, implying that normal wintertime wind stress alone is not sufficient to make the Kuroshio invade the SCS.

[14] Does the wind stress curl also play a role in triggering the intrusion? There are usually two wind stress curls with opposite signs around the Luzon Strait during wintertime (e.g., Figure 6a). Figure 6a shows a positive wind stress curl off northwest Luzon and a negative wind stress curl off southwest Taiwan. The northeast monsoon shielded by the Luzon Island often generates a positive curl off northwest Luzon, whereas another negative curl off southwest Taiwan is due to the wind shielded by the island of Taiwan. The fact that the southern curl (off northwest Luzon) or the northern curl (off southwest Taiwan) or both may favor the Kuroshio intrusion deserves further exploration. *Liang et al.* [2008] suggested the southern wind stress curl would generate a low sea-surface height west

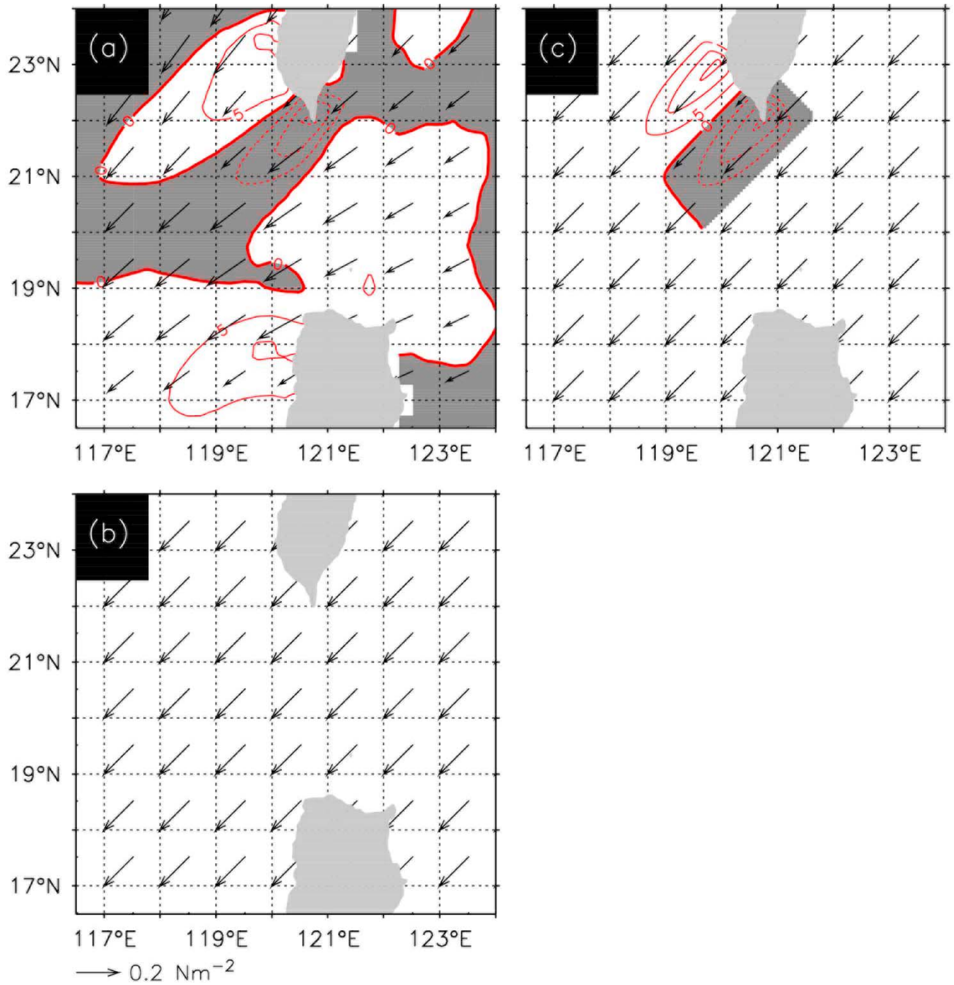

Figure 6. (a) Mean satellite-based wind field during winter, averaged over November–January of 9-year period from 2000 to 2008. (b) Simplified wintertime wind field with spatially homogeneous speed of 0.2 Nm^{-2} from the northeast. (c) Wind stress curl off southwest Taiwan is added to the constant wind field of Figure 6b. Red contour is wind stress curl, and contour interval is 5×10^{-7} Nm^{-3}.

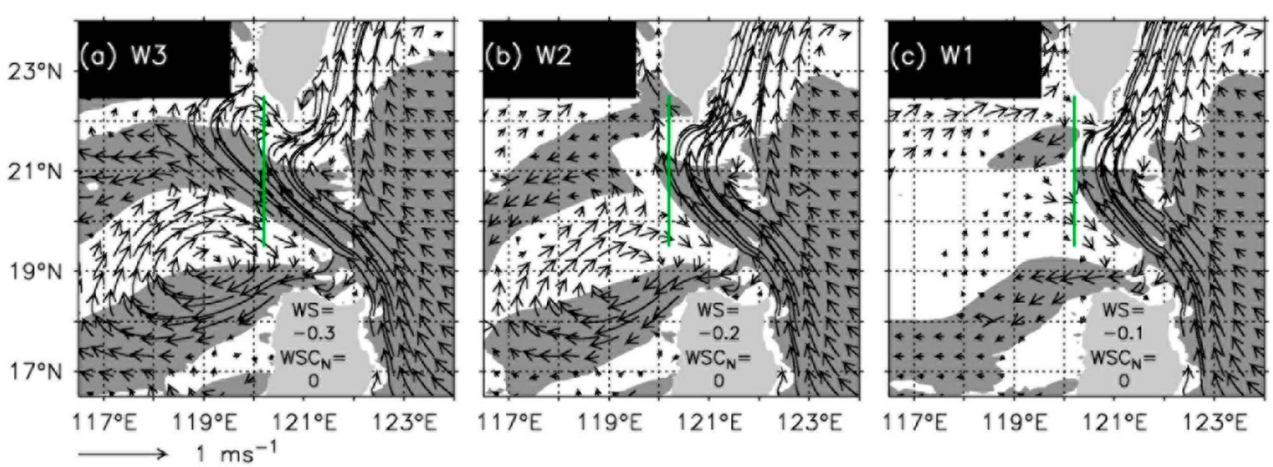

Figure 7. Surface flow patterns for (a) Experiment W3, (b) Experiment W2, and (c) Experiment W1. Surface current is averaged from 0 to 50 m, and only current speed larger than 0.05 ms^{-1} is plotted. Gray shading denotes the westward velocity larger than 0.05 ms^{-1}.

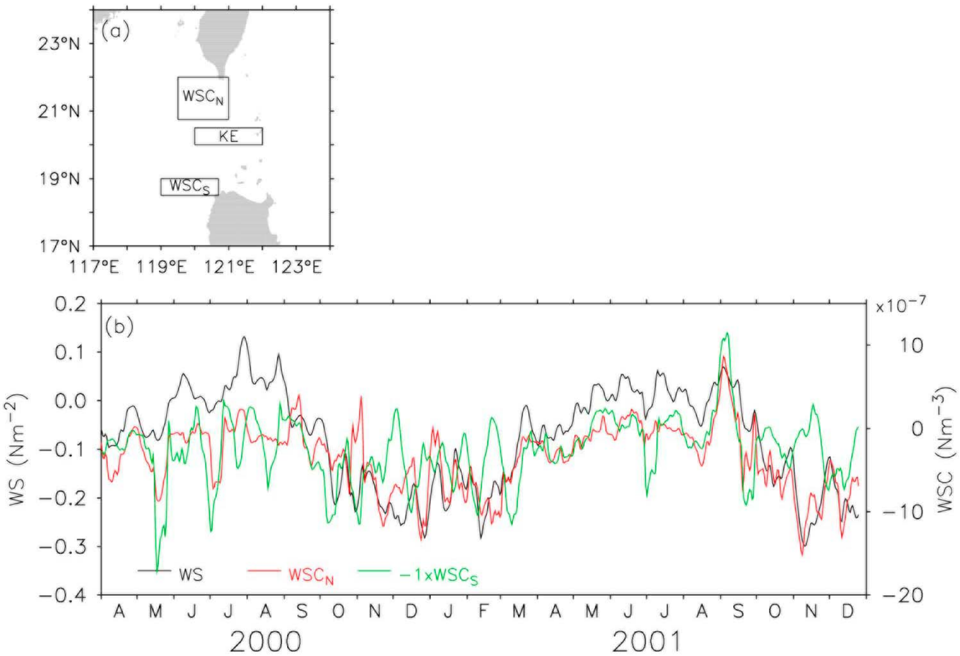

Figure 8. (a) Domains for calculating WSC_N, WSC_S and kinetic energy of the Kuroshio intrusion. (b) Time series of satellite-borne wind stress (rotated in the direction of 45°, black line) together with wind stress curl off southwest Taiwan (WSC_N, red line) and northwest Luzon (WSC_S, green line). Wind stress is averaged over (117°E–123°E, 17°N–23°N). WSC_N and WSC_S are averaged over (119.5°E–121°E, 20.75°N–22°N) and (119°E–120.7°E, 18.5°N–19°N), respectively.

of the Luzon Island, producing a meridional pressure gradient across the Luzon Strait farther south and thus triggering the Kuroshio intrusion into the SCS. Nevertheless, our study reaches a different conclusion.

[15] Figure 8 shows time series of wind stress (rotated 45°), based on data from satellite-borne instruments, together with wind stress curl off southwest Taiwan and northwest Luzon (denoted as WSC_N and WSC_S hereafter). The domain of WSC_S (119°E∼120.7°E and 18.5°N∼19°N) follows *Liang et al.* [2008], who suggested that variation in the Kuroshio intrusion is mainly caused by the wind stress curl variability off northwest Luzon. We adopted 6-hourly maps of 10-m wind component, derived from the QuikSCAT/NCEP blended wind product. The wind stress in the vicinity of Luzon Strait (117°E∼123°E, 17°N∼23°N) is closely correlated with WSC_N (R = 0.80), but not with WSC_S (R = −0.37). The KE (as defined above) is also closely related to WSC_N (R = −0.75), but a low correlation exists between the WSC_S and KE (R = 0.31). This suggests that the wind stress favors a negative WSC_N, whereas the northern curl plays a major role in triggering the Kuroshio intrusion into the SCS.

[16] Experiment W2 was set up with a spatially homogeneous speed of 0.2 Nm^{-2} from the northeast with no wind stress curl (as shown in Figure 6b). The model simulation in Figure 7b shows that the Kuroshio intrusion was confined within the Luzon Strait east of 120°E, and most of the Kuroshio waters returned to the east, flowing northward

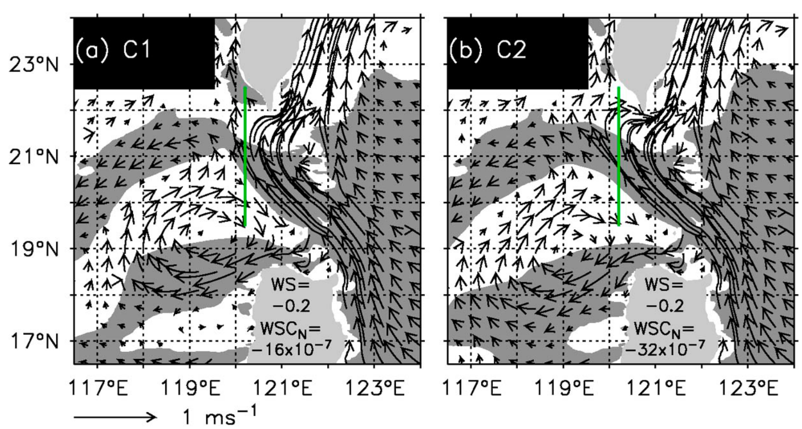

Figure 9. Same as Figure 7, but for (a) Experiment C1 and (b) Experiment C2.

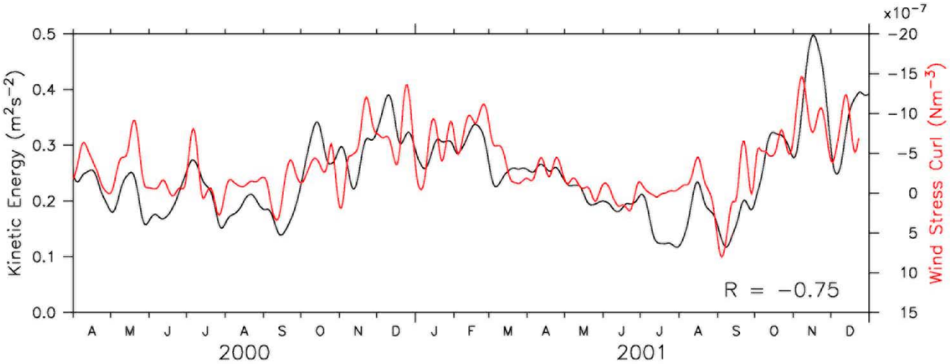

Figure 10. Comparison between WSC_N (red curve) and depth-averaged kinetic energy (0–200 m) of the Kuroshio intrusion (black curve). The areas for calculating WSC_N and kinetic energy are shown in Figure 8a.

along eastern Taiwan. This winter flow pattern differed from that of CTL in Figure 2c, which shows that the Kuroshio made a significant westward encroachment, penetrating into the SCS and extending to 117°E. The only difference in model design between experiments W2 and CTL is the driving wind-forcing. Both of them maintained similar wind intensity on average (about -0.2 Nm^{-2} in winter), but with homogeneous and realistic wind fields, respectively. The results indicate that wind stress curl plays a critical role. Therefore, additional experiments were performed to further demonstrate the contribution of the wind stress curl off southwest Taiwan (WSC_N).

[17] Experiment C1 added additional wind stress curl off southwest Taiwan, with a typical winter value of -1.6×10^{-6} Nm^{-3}, to the constant wind field. The artificial wind field, including spatially homogeneous wind stress of -0.2 Nm^{-2} and the wind stress curl off southwest Taiwan (WSC_N), is shown in Figure 6c. Figure 9a shows the simulation, where the Kuroshio not only intrudes into the Luzon Strait but also penetrates westward into the SCS. This Kuroshio behavior is closer to that in CTL (Figure 2c) than seen in experiment W2 (Figure 7b). The model experiment confirmed that the wind stress curl (WSC_N) is essential to trigger Kuroshio intrusion into the SCS. Experiment C2 doubles the value of WSC_N to -3.2×10^{-6} Nm^{-3}. The intense WSC_N drive more Kuroshio water into the SCS (Figure 9b). A negative WSC_N raises sea level locally. Based on geostrophy, the flow moves around the raised sea level dome along its southern flank, further triggering Kuroshio intrusion.

4. Discussion

[18] In addition to the spatial distribution of the intrusion, the temporal variability between WSC_N and the Kuroshio intrusion is compared in Figure 10. The WSC_N between 119.5°E∼121°E and 20.75°N∼22°N (see Figure 8a) was calculated from QuikSCAT/NCEP blended wind fields. The curl varied both seasonally and intraseasonally. In general, in winter (December–February), the curl was large and negative, whereas it was smaller or even had a positive value in summer. The KE of the Kuroshio intrusion is superimposed in Figure 10 (KE_{KI}, black curve). The KE_{KI} was calculated between 120°E∼122°E and 20°N∼20.5°N (see Figure 8a), which roughly coincides with the Balintang Channel, where the largest westward Kuroshio intrusion occurs [e.g., *Liang et al.*, 2003; *Centurioni et al.*, 2004]. The two time series were consistent, with a correlation coefficient of -0.75, which is higher than the 99% significance level. However, the KE_{KI} was not related to the WSC_S (figure not shown). As mentioned earlier, the domain for calculating WSC_S followed *Liang et al.* [2008], who demonstrated that the Kuroshio intrusion variability was mainly caused by fluctuations in wind stress curl off northwest Luzon. The correlation coefficient between WSC_S and KE_{KI} was 0.31, far below the 99% significant level. Intuitively, both the negative WSC_N and positive WSC_S were favorable for the Kuroshio intrusion into the SCS. However, our analyses demonstrate that only the WSC_N (off southwest Taiwan) played a prominent role in inducing the Kuroshio intrusion. The large and negative WSC_N raised sea level locally, which produced a meridional pressure gradient across the Luzon Strait (lower to the south). This extended the Kuroshio intrusion into the SCS. The WSC_S (off northwest Luzon) could have helped, but it was not chiefly responsible for generating the intrusion. It makes sense that the largest Kuroshio intrusion was mainly northwestward [e.g., *Centurioni et al.*, 2004], as it entered the region of northern wind stress curl influence.

[19] Besides seasonal variation, KE_{KI} also contained intraseasonal fluctuations. KE_{KI} was not strong until early December 2000, when it exceeded 0.35 m^2 s^{-2}. It weakened in early January 2001 and reached another maximum in late February 2001. The peak weakened thereafter. In other words, the Kuroshio intrusion varied from month to month, even during winter. This scenario was confirmed by two subsurface moorings deployed in this region from October 2000 to April 2001. Although the negative WSC_N (off southwest Taiwan) became stronger in December 2000, it contributed to an anticyclonic circulation because the curl provided negative vorticity to the current [*Wu et al.*, 2005]. The enhanced anticyclonic circulation in turn helped the development of the Kuroshio intrusion. The Kuroshio intruded westward into the SCS. The intruded current could probably be regarded as the southern flank of the anticyclonic loop current. However, although the WSC_N weakened in January 2001, the intruded current was prohibited by a weak cyclonic eddy. As the WSC_N was enhanced again in

February 2001, the intruded current was strengthened by the large vorticity from the curl. The close consistency between the WSC_N and the observed velocity field (and/or the model's intruded kinetic energy) suggests that the curl off southwest Taiwan was a major factor in triggering intra-seasonal variation in the Kuroshio intrusion.

5. Concluding Remarks

[20] We used an observation-validated, three-dimensional model to study the forcing mechanism leading to the Kuroshio intrusion into the SCS. The model simulation reproduced the seasonal patterns of the Kuroshio intrusion. The Kuroshio intrusion wanes in summer, and the intrusion is mainly confined within a well-rounded Kuroshio meander. During winter the water intrudes farther into the SCS, extending to 117°E. The concurrent altimeter-based geostrophic velocities lend support to the present model. By careful design of model experiments, we demonstrated that wind inside the SCS is relatively important for the Kuroshio intrusion.

[21] The upstream Kuroshio intensity in the Luzon Strait is related to the intrusion. An intense winter monsoon reinforces the upstream Kuroshio, enhancing the Kuroshio intrusion into the SCS. The wind stress curl off southwest Taiwan (WSC_N) also has a significant impact on the Kuroshio intrusion. The wind stress curl off northwest Luzon (WSC_S) may help, but it is not chiefly responsible for generating the intrusion. The Kuroshio intrusion has both seasonal and intraseasonal variations. The variations are consistent with the variability of wind stress curl off southwest Taiwan, further indicating that WSC_N is the dominant forcing. As the local negative wind stress curl strengthens, the region tends to form an anticyclonic circulation, acquiring vorticity from the wind curl. The enhanced anticyclonic circulation then facilitates the westward intrusion of the Kuroshio.

[22] This study was focused on identifying the wind-related forcing regulating the Kuroshio intrusion. However, several other mechanisms may also contribute. For example, the degree of Kuroshio intrusion could be a function of the upstream state of the Kuroshio. Westward-propagating eddies from the Pacific may have impacts on the Kuroshio in the Luzon Strait, causing intrusion variability [e.g., *Sheu et al.*, 2010]. Sea-surface height differences between the western Pacific and the SCS have an important effect on the upper-layer transport through the Luzon Strait [*Song*, 2006]. Baroclinic instability of the Kuroshio front in the Luzon Strait may also affect intrusion behavior. Including the wind-related forcing, all of these mechanisms may be inter-related, with changes in one affecting the others. These complicated features deserve to be further explored and will be studied in the near future.

[23] **Acknowledgments.** The authors would like to thank the three anonymous reviewers for their careful review of the manuscript and detailed suggestions to improve the manuscript. This research was supported by the National Science Council, Taiwan, ROC, under grants NSC 100-2628-M-003-001.

References

Centurioni, L. R., P. P. Niller, and D.-K. Lee (2004), Observations of inflow of Philippine Sea surface water into the South China Sea through the Luzon Strait, *J. Phys. Oceanogr.*, *34*, 113–121, doi:10.1175/1520-0485(2004)034<0113:OOIOPS>2.0.CO;2.

Farris, A., and M. Wimbush (1996), Wind-induced intrusion into the South China Sea, *J. Oceanogr.*, *52*, 771–784, doi:10.1007/BF02239465.

Hsin, Y.-C., C.-R. Wu, and P.-T. Shaw (2008), Spatial and temporal variations of the Kuroshio east of Taiwan, 1982–2005: A numerical study, *J. Geophys. Res.*, *113*, C04002, doi:10.1029/2007JC004485.

Hsin, Y.-C., T. Qu, and C.-R. Wu (2010), Intra-seasonal variation of the Kuroshio southeast of Taiwan and its possible forcing mechanism, *Ocean Dyn.*, *60*, 1293–1306, doi:10.1007/s10236-010-0294-2.

Hsin, Y.-C., C.-R. Wu, and S.-Y. Chao (2012), An updated examination of the Luzon Strait transport, *J. Geophys. Res.*, *117*, C03022, doi:10.1029/2011JC007714.

Jia, Y., and E. P. Chassignet (2011), Seasonal variation of eddy shedding from the Kuroshio intrusion in the Luzon Strait, *J. Oceanogr.*, *67*, 601–611, doi:10.1007/s10872-011-0060-1.

Liang, W.-D., T. Y. Tang, Y. J. Yang, M. T. Ko, and W.-S. Chuang (2003), Upper-ocean currents around Taiwan, *Deep Sea Res., Part II*, *50*, 1085–1105, doi:10.1016/S0967-0645(03)00011-0.

Liang, W.-D., Y. J. Yang, T. Y. Tang, and W.-S. Chuang (2008), Kuroshio in the Luzon Strait, *J. Geophys. Res.*, *113*, C08048, doi:10.1029/2007JC004609.

Mellor, G. L. (2004), Users guide for a three-dimensional, primitive equation, numerical ocean model, report, 56 pp., Program in Atmos. and Oceanic Sci., Princeton Univ., Princeton, N. J.

Metzger, E. J., and H. E. Hurlburt (1996), Coupled dynamics of the South China Sea, the Sulu Sea, and the Pacific Ocean, *J. Geophys. Res.*, *101*, 12,331–12,352, doi:10.1029/95JC03861.

Metzger, E. J., and H. E. Hurlburt (2001a), The importance of high horizontal resolution and accurate coastline geometry in modeling South China Sea inflow, *Geophys. Res. Lett.*, *28*, 1059–1062, doi:10.1029/2000GL012396.

Metzger, E. J., and H. E. Hurlburt (2001b), The nondeterministic nature of Kuroshio penetration and eddy shedding in the South China Sea, *J. Phys. Oceanogr.*, *31*, 1712–1732, doi:10.1175/1520-0485(2001)031<1712:TNNOKP>2.0.CO;2.

Nan, F., H. Xue, F. Chai, L. Shi, M. Shi, and P. Guo (2011), Identification of different types of Kuroshio intrusion into the South China Sea, *Ocean Dyn.*, *61*, 1291–1304, doi:10.1007/s10236-011-0426-3.

Qu, T. (2000), Upper-layer circulation in the South China Sea, *J. Phys. Oceanogr.*, *30*, 1450–1460, doi:10.1175/1520-0485(2000)030<1450:ULCITS>2.0.CO;2.

Qu, T., H. Mitsudera, and T. Yamagata (2000), Intrusion of the North Pacific waters into the South China Sea, *J. Geophys. Res.*, *105*, 6415–6424, doi:10.1029/1999JC900323.

Rio, M. H., P. Schaeffer, G. Moreaux, J. M. Lemoine, and E. Bronner (2009), A new mean dynamic topography computed over the global ocean from GRACE data, altimetry and in situ measurements, paper presented at OceanObs09 Conference, Eur. Space Agency, Venice, Italy, 21–25 Sep.

Shaw, P.-T. (1989), The intrusion of water masses into the sea southwest of Taiwan, *J. Geophys. Res.*, *94*, 18,213–18,226, doi:10.1029/JC094iC12p18213.

Shaw, P.-T. (1991), The seasonal variation of the intrusion of the Philippine Sea water into the South China Sea, *J. Geophys. Res.*, *96*, 821–827, doi:10.1029/90JC02367.

Sheremet, V. A. (2001), Hysteresis of a western boundary current leaping across a gap, *J. Phys. Oceanogr.*, *31*, 1247–1259, doi:10.1175/1520-0485(2001)031<1247:HOAWBC>2.0.CO;2.

Sheu, W.-J., C.-R. Wu, and L.-Y. Oey (2010), Blocking and Westward Passage of eddies in the Luzon Strait, *Deep Sea Res., Part II*, *57*, 1783–1791, doi:10.1016/j.dsr2.2010.04.004.

Song, Y. T. (2006), Estimation of interbasin transport using ocean bottom pressure: Theory and model for Asian marginal seas, *J. Geophys. Res.*, *111*, C11S19, doi:10.1029/2005JC003189.

Wu, C.-R., and Y.-C. Hsin (2005), Volume transport through the Taiwan Strait: A numerical study, *Terr. Atmos. Oceanic Sci.*, *16*(2), 377–391.

Wu, C.-R., T. Y. Tang, and S. F. Lin (2005), Intra-seasonal variation in the velocity field of the northeastern South China Sea, *Cont. Shelf Res.*, *25*, 2075–2083, doi:10.1016/j.csr.2005.03.005.

Wu, C.-R., H.-F. Lu, and S.-Y. Chao (2008), A numerical study on the formation of upwelling off northeast Taiwan, *J. Geophys. Res.*, *113*, C08025, doi:10.1029/2007JC004697.